Imaging through turbid layers by scanning the phase conjugated second harmonic radiation from a nanoparticle

Chia-Lung Hsieh,[1,2*] Ye Pu,[1] Rachel Grange,[1] Grégoire Laporte,[1] and Demetri Psaltis[1]

[1]*School of Engineering, EPFL, Station 17, 1015 Lausanne, Switzerland*
[2]*Department of Electrical Engineering, California Institute of Technology, 1200 East California Boulevard, MC 136-93, Pasadena, California 91125, USA*
**chia-lung.hsieh@epfl.ch*

Abstract: We demonstrate imaging through a turbid layer by using digital phase conjugation of the second harmonic field radiated from a beacon nanoparticle. We show that the phase-conjugated focus can be displaced from its initial position by illuminating the same region of the turbid layer with an angular offset. An image is obtained by scanning the phase-conjugated focus through the turbid layer in a region around the nanoparticle. We obtain a clear image of the target by measuring the light transmitted through it when scanning the focused beam.

OCIS codes: (070.5040) Phase conjugation; (090.1995) Digital holography; (110.0113) Imaging through turbid media; (160.4236) Nanomaterials; (160.4330) Nonlinear optical materials; (180.5810) Scanning microscopy.

References and links

1. J. W. Goodman, W. H. Huntley, D. W. Jackson, and M. Lehmann, "Wavefront-reconstruction imaging through random media," Appl. Phys. Lett. **8**(12), 311–313 (1966).
2. E. N. Leith, and J. Upatniek, "Holographic imagery through diffusing media," J. Opt. Soc. Am. **56**(4), 523 (1966).
3. H. Kogelnik, and K. S. Pennington, "Holographic imaging through a random medium," J. Opt. Soc. Am. **58**(2), 273–274 (1968).
4. I. M. Vellekoop, and A. P. Mosk, "Focusing coherent light through opaque strongly scattering media," Opt. Lett. **32**(16), 2309–2311 (2007).
5. I. M. Vellekoop, and A. P. Mosk, "Universal optimal transmission of light through disordered materials," Phys. Rev. Lett. **101**(12), 120601 (2008).
6. Z. Yaqoob, D. Psaltis, M. S. Feld, and C. Yang, "Optical phase conjugation for turbidity suppression in biological samples," Nat Photonics **2**(2), 110–115 (2008).
7. M. Cui, E. J. McDowell, and C. H. Yang, "An in vivo study of turbidity suppression by optical phase conjugation (TSOPC) on rabbit ear," Opt. Express **18**(1), 25–30 (2010).
8. M. Cui, and C. H. Yang, "Implementation of a digital optical phase conjugation system and its application to study the robustness of turbidity suppression by phase conjugation," Opt. Express **18**(4), 3444–3455 (2010).
9. C. L. Hsieh, Y. Pu, R. Grange, and D. Psaltis, "Digital phase conjugation of second harmonic radiation emitted by nanoparticles in turbid media," Opt. Express **18**(12), 12283–12290 (2010).
10. I. M. Vellekoop, A. Lagendijk, and A. P. Mosk, "Exploiting disorder for perfect focusing," Nat. Photonics **4**(5), 320–322 (2010).
11. T. Čižmár, M. Mazilu, and K. Dholakia, "In situ wavefront correction and its application to micromanipulation," Nat. Photonics **4**(6), 388–394 (2010).
12. J. W. Goodman, and R. W. Lawrence, "Digital image formation from electronically detected holograms," Appl. Phys. Lett. **11**(3), 77–79 (1967).
13. F. Mok, J. Diep, H. K. Liu, and D. Psaltis, "Real-time computer-generated hologram by means of liquid-crystal television spatial light modulator," Opt. Lett. **11**(11), 748–750 (1986).
14. C. L. Hsieh, R. Grange, Y. Pu, and D. Psaltis, "Three-dimensional harmonic holographic microcopy using nanoparticles as probes for cell imaging," Opt. Express **17**(4), 2880–2891 (2009).
15. J. Extermann, L. Bonacina, E. Cuña, C. Kasparian, Y. Mugnier, T. Feurer, and J.-P. Wolf, "Nanodoublers as deep imaging markers for multi-photon microscopy," Opt. Express **17**(17), 15342–15349 (2009).

#132231 - $15.00 USD Received 26 Jul 2010; revised 5 Sep 2010; accepted 8 Sep 2010; published 15 Sep 2010

16. C. L. Hsieh, R. Grange, Y. Pu, and D. Psaltis, "Bioconjugation of barium titanate nanocrystals with immunoglobulin G antibody for second harmonic radiation imaging probes," Biomaterials **31**(8), 2272–2277 (2010).
17. I. M. Vellekoop, and C. M. Aegerter, "Scattered light fluorescence microscopy: imaging through turbid layers," Opt. Lett. **35**(8), 1245–1247 (2010).
18. I. Freund I, M. Rosenbluh, and S. Feng, "Memory effects in propagation of optical waves through disordered media," Phys. Rev. Lett. **61**(20), 2328–2331 (1988).
19. Y. Pu, M. Centurion, and D. Psaltis, "Harmonic holography: a new holographic principle," Appl. Opt. **47**(4), A103–A110 (2008).
20. E. Shaffer, N. Pavillon, J. Kühn, and C. Depeursinge, "Digital holographic microscopy investigation of second harmonic generated at a glass/air interface," Opt. Lett. **34**(16), 2450–2452 (2009).
21. O. Masihzadeh, P. Schlup, and R. A. Bartels, "Label-free second harmonic generation holographic microscopy of biological specimens," Opt. Express **18**(10), 9840–9851 (2010).
22. E. Shaffer, P. Marquet, and C. Depeursinge, "Real time, nanometric 3D-tracking of nanoparticles made possible by second harmonic generation digital holographic microscopy," Opt. Express **18**(16), 17392–17403 (2010).
23. M. Zielinski, D. Oron, D. Chauvat, and J. Zyss, "Second-harmonic generation from a single core/shell quantum dot," Small **5**(24), 2835–2840 (2009).
24. Y. Pu, R. Grange, C. L. Hsieh, and D. Psaltis, "Nonlinear optical properties of core-shell nanocavities for enhanced second-harmonic generation," Phys. Rev. Lett. **104**(20), 207402 (2010).
25. P. R. Seem, J. D. R. Buchanan, and R. P. Cowburn, "Impact of surface roughness on laser surface authentication signatures under linear and rotational displacements," Opt. Lett. **34**(20), 3175–3177 (2009).
26. S. Feng, C. Kane, P. A. Lee, and A. D. Stone, "Correlations and fluctuations of coherent wave transmission through disordered media," Phys. Rev. Lett. **61**(7), 834–837 (1988).

1. Introduction

Imaging through turbid media has been recognized as a highly desirable capability, but its implementation remains challenging. Several optical techniques have been developed to achieve imaging through turbid media [1–11]. Optical phase conjugation is one of the techniques that have been proposed [1–3,6–9]. Recently, it has been demonstrated that phase conjugation can be performed all digitally [8,9] by combining digital holography [12] with dynamic computer generated holography [13]. We have used Digital Phase Conjugation (DPC) to focus light through a stationary turbid medium by using a Second Harmonic Radiation IMaging Probe (SHRIMP) [14–16] as a beacon [9]. In a typical DPC, a coherent SHG point source is placed inside the turbid sample and the complex scattered field is recorded by digital holography. The phase-conjugated scattered field is then generated by a spatial light modulator (SLM) and sent back to the sample. The turbid medium undoes the scattering and focuses the phase-conjugated light at the position where the coherent light source was initially placed. Compared with other wave front correction techniques, DPC shows promise as a fast and efficient technique because the phase-conjugated beam is adapted to the recorded scattered field without the need for lengthy iterative optimization calculations.

Wave front correction allows us to form a nearly optimal focus inside a turbid sample, but a loftier goal is to image an object that is behind the scattering medium. Recently, Vellekoop and Aegerter [17] have demonstrated a method for producing fluorescence images of objects behind diffusing screens by scanning a beam that is focused through the turbid media using wave front optimization. In this paper, we demonstrate the use of DPC rather than wave front optimization to achieve this goal. The main benefit of DPC is its speed of finding the tailored wave front since no iterative optimization calculations are necessary. With sufficiently bright SHRIMPs, the speed is determined by the response time of the SLM which needs to be reconfigured only once with DPC. On the contrary, wave front optimization requires a large number of sequential modulations of the SLM to find the optimal wave front. Therefore, DPC has an inherent advantage in speed.

2. Principles

The method we used for imaging through turbid media consists of two steps: (1) measurement of the local response of the turbid sample by holographically recording the complex scattered field emitted from a coherent point source; (2) scanning the phase-conjugated focus on the

#132231 - $15.00 USD Received 26 Jul 2010; revised 5 Sep 2010; accepted 8 Sep 2010; published 15 Sep 2010

sample and measuring the transmitted field to form an image. The first step is depicted in Fig. 1 (a). A SHRIMP at $z = 0$ emits SHG field as a coherent dipole point source. The role of the SHRIMP in this approach can be seen as a beacon of the focusing light: the SHRIMP helps us find the tailored wave front for focusing light around it. The SHG emission is close to a spherical wave in the far field. The SHG emission propagates in free space and is then scattered by the turbid medium placed at a distance $z = D$. The scattered field is recorded by digital hologram where the complex field information is captured. This information can be seen as the local response of the turbid medium corresponding to the input of a spherical wave.

In the second step, the phase-conjugated field is recreated from the recorded hologram using a phase-only SLM. The phase-conjugated scattered field is then sent back to the sample as shown in Fig. 1 (b). The turbid medium undoes the initial scattering and a phase-conjugated focus forms at the position where the SHRIMP is initially placed. To achieve imaging with the phase-conjugated focus, it is critical to have the capability of moving the focus away from its initial position.

Consider the situation in Fig. 1 (b) where the phase-conjugated beam is tilted and illuminates the same region where the local response has been characterized (shown as the red circular region). When the tilt angle is small and the turbid medium is thin, the phase-conjugated beam will pass through almost identical (i.e., highly correlated) portions of the perturbing medium [1,18]. As a result, the turbid medium will cancel the wave front distortion, and a tilted converging beam can be obtained right behind the turbid medium. We found that the best results were obtained by ensuring that the phase-conjugated beam passes through the same region on the scattering medium while scanning. This requires that the illuminating beam is swept and simultaneously shifted so the light beam pivots around the same illumination region on the turbid medium.

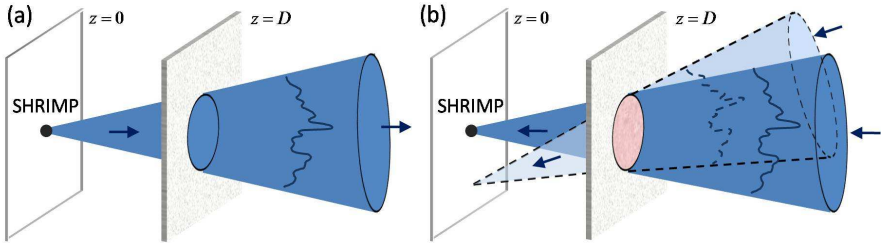

Fig. 1. Two steps of imaging through turbid media in a phase-conjugate scanning microscopy. (a) Recording the scattered SHG field radiated from a SHRIMP by digital holography. (b) Scanning the phase-conjugated focus on the imaging plane by illuminating the same region of the turbid medium (shown as the red circular region) with the phase-conjugated beam at different angles.

3. Experiments

The turbid medium is a commercial ground glass diffuser (Edmund Optics, NT43-723). We prepared an object consisting of gold thin film patterns (130-nm thick) on a transparent glass substrate (150-μm thick) by standard photolithography. We used 300-nm (in diameter) barium titanate ($BaTiO_3$) nanoparticles as the SHRIMPs. The crystal structure of the $BaTiO_3$ nanoparticles is tetragonal which is non-centrosymmetric and allows for efficient SHG. The SHRIMPs were deposited randomly on the image target.

The experimental setup is shown in Fig. 2. The excitation light source was a Ti:sapphire oscillator generating 150 fs laser pulses at 80 MHz centered at 800 nm. The excitation was focused by a 10x microscope objective (NA 0.25, OBJ1 in Fig. 2 (a)) onto a SHRIMP which was located at a transparent area of the target. The average excitation power was approximately 50 mW. The SHG signal from the SHRIMP emits in both forward and backward directions. The backward SHG signal was collected by the same microscope

#132231 - $15.00 USD Received 26 Jul 2010; revised 5 Sep 2010; accepted 8 Sep 2010; published 15 Sep 2010

objective (OBJ1) and then imaged on a charge-coupled device (CCD) camera (Scion, CFW-1312M, CCD1 in Fig. 2) with a lens of 20-cm focal length (L1). The forward SHG signal was scattered by the diffuser after propagating by approximately 2 mm (the working distance of the OBJ2). The scattered SHG field was recorded by a harmonic holographic (H^2) microscope [14,19–22]. The H^2 microscope can be understood as a 4F imaging system followed by a holographic recording system. The scattered SHG field from the SHRIMP is collected and optically magnified by a 4F system consisting of a 10x microscope objective (NA 0.25, OBJ2 in Fig. 2) and a lens with 20 cm focal length (L2). The detector of the H^2 microscope is an electron multiplying charge coupled device (EMCCD, Andor iXonEM + 885) camera (CCD2 in Fig. 2). We placed the CCD2 away from the 4F imaging plane so that the scattered field could propagate and fill the detection area of the EMCCD. The hologram recording distance, i.e. the distance between the SHG image formed by the 4F system and the EMCCD, is 20 cm. A plane wave at the SHG frequency generated by a separate BBO crystal served as the reference beam. By overlapping the scattered field and reference beam both spatially and temporally on the CCD2, we record an off-axis digital hologram of the scattered SHG field. The angle between the signal and reference arms was about 1 degree. The complex scattered SHG field is then extracted from the recorded off-axis digital hologram.

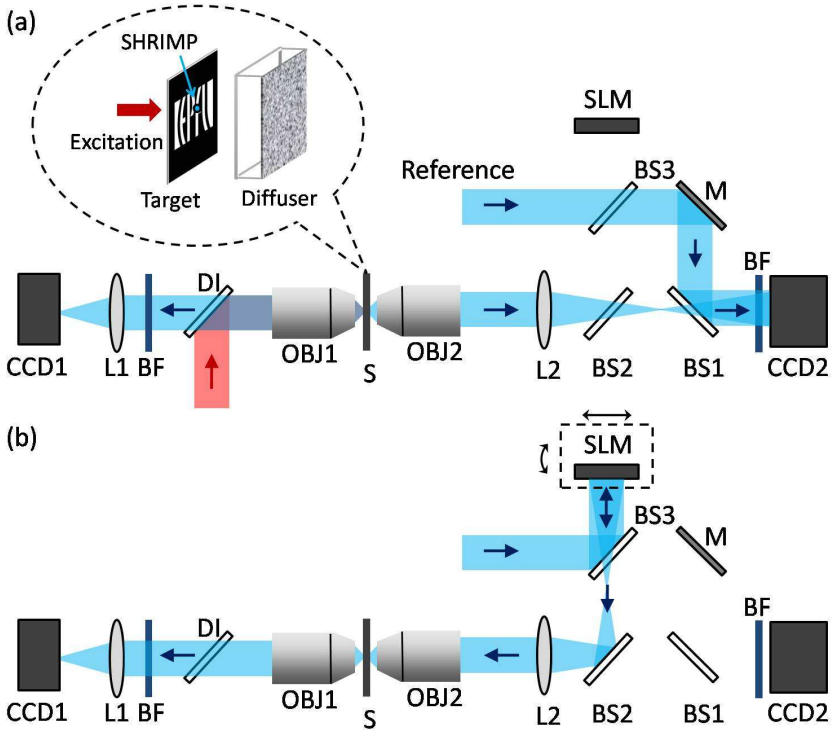

Fig. 2. (a) The experimental setup of the harmonic holographic microscopy for recording the complex scattered SHG field. Inset: The illustrative diagram of the sample structure. (b) The experimental setup of the phase-conjugate scanning microscope. Note that (a) and (b) show the same setup with different light illuminations for different steps of the experiment. The light not in use is blocked in the experiment and is not shown in the figures. DI, dichroic mirror; L1 – L4, lens; OBJ1 and OBJ2, microscope objectives; S, sample; BS1 – BS3, non-polarizing beam splitters; BF, band-pass filter centered at 400 nm; M, mirror.

The second part of the experiment is to produce the phase-conjugated focus and to scan it on the sample for imaging as shown in Fig. 2 (b). We digitally conjugated the measured phase of the scattered field and projected it on to a phase-only reflective SLM (PLUTO-VIS, HOLOEYE). The pixel size of the SLM is 8 x 8 μm^2, which matches with the pixel size of the

#132231 - $15.00 USD Received 26 Jul 2010; revised 5 Sep 2010; accepted 8 Sep 2010; published 15 Sep 2010

CCD2. A plane wave at the SHG frequency is incident on the SLM and picks up the conjugated phase pattern after the reflection. The phase-conjugated beam is delivered back to the turbid medium through the 4F system. When the optical system is well aligned (i.e. the CCD2 and the SLM are aligned pixel by pixel), the turbid medium undoes the scattering and the phase-conjugated beam forms a focus on the SHRIMP. The quality of the phase-conjugated focus can be evaluated with the imaging system consisted of the OBJ1, L1 and CCD1.

The scanning of the phase-conjugated focus is achieved by tilting and shifting the SLM simultaneously. The SLM position has six degrees of freedom in space, including three translational directions (two are in-plane lateral and one is axial), two tilt directions (vertical and horizontal), and one in-plane rotation. In our demonstration, the two lateral shift adjustments of the SLM are controlled by two motorized stages, and the two tilt adjustments are controlled by two motorized actuators assembled on a tilt platform. Scanning the phase-conjugated focus can be achieved by rotating the beam around the same region of the turbid medium as a pivot (as shown in Fig. 1 (b)), which generally requires a coordination between the tilt and the shift of the SLM. The optical path between the SLM and the lens L2 (20 cm focal length) is 40 cm. This distance is identical to the distance between the CCD2 and the lens L2. As a result, the image of the SLM forms between the focal plane and the OBJ2 as shown in Fig. 3 (a). When the SLM is tilted, this SLM image will tilt accordingly (with an optical magnification due to the 4F system) as shown in Fig. 3 (b). In Fig. 3 (b), it is clear that, after the tilt, the phase-conjugated beam traverses different regions (shown as dashed circles) from the original path (shown as solid circles). In general, the turbid medium is not placed at the SLM image plane and therefore it is necessary to shift the SLM image correspondingly so that the tilted beam passes through the same region of the turbid medium. It is worth noting that our approach achieves a true pivoting beam, while a conventional two-axis raster scanner results in a pivoting-like beam because the two-axis scanning is done by two separate mirrors. It is also interesting to note that the mechanical tilt and shift of the SLM are equivalent to electronically modulating the phase pattern on the SLM. One would need to calculate a new phase pattern for each specific tilt and shift. The motionless digital scanning may have advantages in some applications where mechanical scan is not allowed.

In order to form the image, we replaced the CCD1 in Fig. 2 (b) by a photomultiplier tube (PMT) and the transmission signal was measured. Therefore, when the phase-conjugated focus falls at a transparent area of the target, the signal obtained from the scanning beam is bright. To increase the sensitivity of the measurement, we modulated the phase-conjugated beam by an optical chopper at 300 Hz, and the signal was demodulated and read out with a lock-in amplifier.

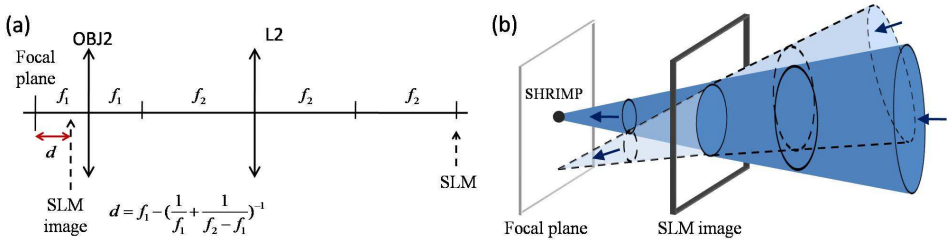

Fig. 3. Illustration of the tilt of the phase-conjugated beam as the SLM tilts. (a) The optical diagram of the SLM projection through the 4F imaging system consisting of L2 and OBJ2. Note that the SLM is not placed at the imaging plane of the 4F system, and therefore the SLM image is between the focal plane and OBJ2. Here f_1 and f_2 are the focal length of the OBJ2 and L2; d is the distance between the focal plane and the SLM image plane. (b) The illustrative diagram showing how the phase-conjugated beam tilts while the SLM tilts. Details of the coordination between the tilt and the shift of the SLM for the scanning are in the main text.

#132231 - $15.00 USD Received 26 Jul 2010; revised 5 Sep 2010; accepted 8 Sep 2010; published 15 Sep 2010

4. Results and discussion

We verified that the diffuser was sufficiently scattering by placing it at the output aperture of the objective and focusing directly through it without phase conjugation. The speckle pattern obtained on the image plane is shown in Fig. 4 (a). To focus through the turbid medium, we performed the phase-conjugation of the scattered SHG field emitted from the SHRIMP. The time for digital holographic recording of the scattered SHG field was 1 second, limited primarily by the CCD integration time. This can be reduced by at least an order of magnitude if more efficient SHRIMPs are used [23,24]. For the purpose of characterization of the optical system, the SHRIMPs were randomly deposited on a glass substrate instead of a target. The conjugated random phase pattern (as shown in Fig. 4 (b)) is projected on the SLM for generating a phase-conjugated beam. When the phase-conjugated beam illuminated the turbid medium, a sharp focus was observed as shown in Fig. 4 (c). The full-width-half-maximum (FWHM) of the phase-conjugated focus is 2 μm which is the diffraction limit of the optical system. The average intensity within the FWHM of the phase-conjugated focus is approximately 400 times greater than the average diffusive background in Fig. 4 (a). Note that Fig. 4 (a) and (c) share the same grayscale except the signal intensity in Fig. 4 (a) is artificially increased by 100 times for better visualization.

We then scanned the focus across on the sample by illuminating the phase-conjugated beam on the same region of the turbid medium at different angles via tilting and shifting the SLM accordingly. In our demonstration, the correspondence between the tilt and the shift of the SLM was typically 270-μm shift per 1-mrad tilt. Note that the tilt of the optical beam is double the tilt of the SLM due to the reflection, and the tilt/shift of the phase-conjugated beam at the sample position is increased/reduced by the 4F imaging system by a factor of the optical magnification. While this coordination is maintained, the phase-conjugated focus can be scanned across the sample. To examine the scanning field of view, we tracked and measured the intensity of the phase-conjugated focus as it scanned across the sample by monitoring it on CCD1 in Fig. 2. The result is shown in Fig. 5. The intensity of the focus remains almost unchanged at small tilt angle, and it decreases by half at a large tilt angle of approximately 55 mrad.

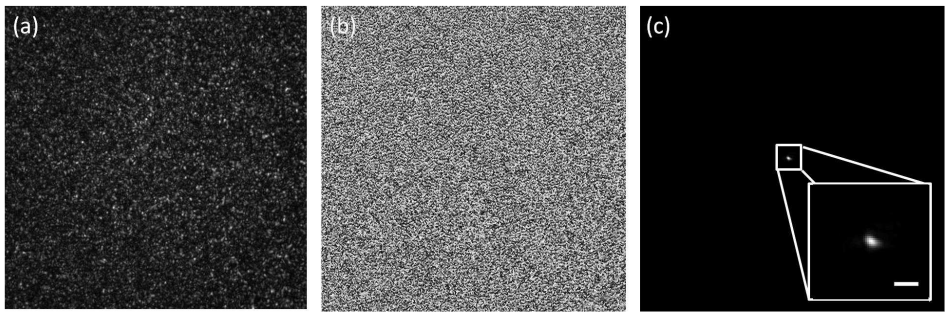

Fig. 4. Focusing through the turbid medium without and with phase conjugation. (a) The speckle pattern on the image plane when focusing directly through the turbid medium by the objective without phase conjugation. (b) The conjugated phase pattern projected on the SLM for phase conjugation. The grayscale from black to white represents the phase modulation from 0 to 2π. (c) The phase-conjugated focus on the image plane. The inset shows the magnified image of the focus. The scale bar in the inset is 5 μm. The size of the images in (a) and (c) is 195 ´195 μm^2.

#132231 - $15.00 USD Received 26 Jul 2010; revised 5 Sep 2010; accepted 8 Sep 2010; published 15 Sep 2010

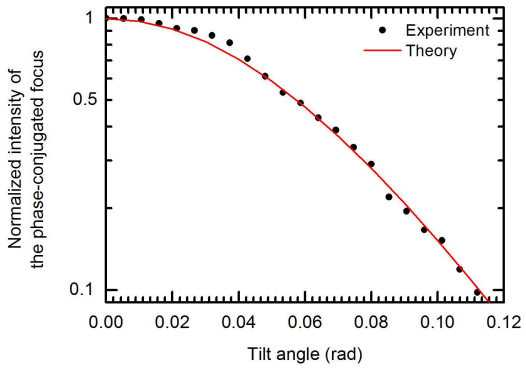

Fig. 5. Angular response of the tilted phase-conjugated focus. Note that the tilt angle in this figure is the tilt angle at the sample position. The experimental data is shown as black dots and the theoretical fitting is shown as the red line.

The reason that the phase-conjugated focus can be displaced from its initial position is based on the fact that the scattering behavior of a thin turbid medium is highly correlated when the incident beam is tilted at a small angle. This phenomenon has been referred to as the "memory effect" and it was studied for different thicknesses of the turbid media [18]. The scattering of the diffuser in our case is due to surface roughness. Therefore the turbid medium is effectively very thin. As a result, the angular range for high correlation in the scattering behavior is large, which allows us to have a large field of view for phase-conjugate scanning microscopy. The diffuser we used in the experiment was a 120-grit ground glass, and it has been reported that the root-mean-square surface roughness of a 120-grit ground glass was 3.1 μm with in-plane characteristic length as 45 μm [25].

Based on the theory of the memory effect, the correlation function $C(qL)$, which is equivalent to the normalized intensity of the phase-conjugated focus, has the form of $C(qL)=\left[qL/\sinh(qL)\right]^2$ where $q=2\pi\delta\theta/\lambda$, $\delta\theta$ is the tilt angle, λ is the optical wavelength, and L is the thickness of the turbid medium [26]. We fit the experimental data in Fig. 5 with the theory (shown as the red line). The experimental observation agrees with the theory very well with the effective thickness L as 1.65 μm.

It should be mentioned that the field of view is also determined by the distance between the turbid medium and the plane of focus of the conjugate beam. In our case, the distance between the turbid medium to the focal plane is approximately 2 mm, leading to a large field of view of 220-μm diameter FWHM. When the turbid medium is directly on top of the focal plane, the field of view in the phase-conjugate scanning microscopy vanishes.

We demonstrate the imaging capability of the phase-conjugate scanning microscopy by using a metal pattern on a glass substrate as the target. The wide-field light transmission image of the target is shown in Fig. 6 (a) where the logo of Ecole Polytechnique Federale de Lausanne (EPFL) can be seen. The SHRIMPs were randomly deposited on the target, and one SHRIMP located at a transparent area was excited from the back of the sample for phase conjugation. The scanning of the phase-conjugated focus was performed by coordinating the tilt and the shift of the SLM as described previously. We scanned the focus across an area of 115 ´ 115 μm^2 on the sample. The transmission signal was collected by the PMT placed at the position of CCD1 in Fig. 2 (b). The integration time for each pixel was 30 ms. The corresponding phase-conjugate scanning image is shown in Fig. 6 (b) where the target is clearly resolved. For comparison, we performed a control experiment without phase conjugation by simply focusing the initial undisturbed spherical wave through the turbid medium on the sample. As expected, the scanning image is very blurry as shown in Fig. 6 (c).

#132231 - $15.00 USD Received 26 Jul 2010; revised 5 Sep 2010; accepted 8 Sep 2010; published 15 Sep 2010

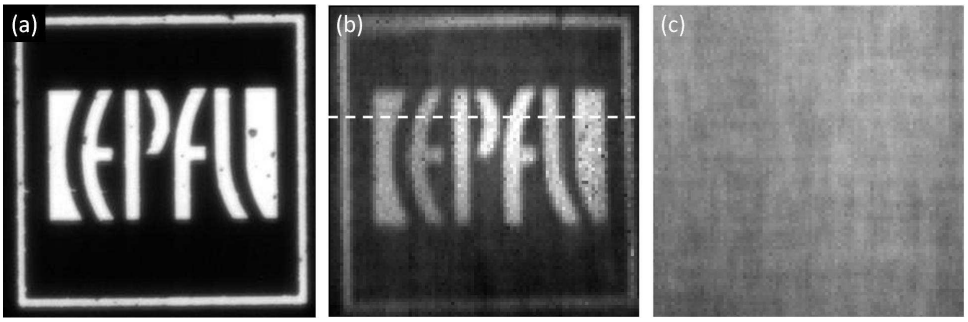

Fig. 6. Phase-conjugate scanning images. (a) The wide-field transmission image of the target. The target is a 130-nm thick gold pattern on a glass substrate prepared by photolithography. The bright region in this figure indicates the transparent area while the dark region indicates the gold film. (b) The corresponding phase-conjugate scanning image of the target. The target is clearly resolved. The intensity profile along the dashed line is plotted in Fig. 7. (c) The scanning image of the same target without phase conjugation. Since the focus is severely distorted by the turbid medium, the image is completely blurry. The size of the images are 115 ´ 115 μm^2.

The intensity profile along the dashed line in Fig. 6 (b) is plotted in Fig. 7. The uniformly sharp image demonstrates that the conjugate spot remains focused as it is scanned. The spatial resolution of the system is 2 μm, determined by the diffraction-limited phase-conjugated focus spot size. The signal intensity gradually drops towards the edges of the image because the intensity of the phase-conjugated focus decreases when the angular offset increases due to the memory effect (as shown in Fig. 5).

We would like to mention that the only image processing for Fig. 6 (b) is a uniform background subtraction. The typical phase-conjugated focus for scanning was shown previously in Fig. 4 (c). The contrast of the focus was high: the peak intensity within the FWHM of the focus was 400 times stronger than the diffusive background. During the scanning, all the light transmitted through the metal pattern was collected by the PMT. Therefore, the total detected power from the diffusive background can be considerable due to the large transparent area on the pattern, which contributes a bias background in the scanning image. This background results in a relatively low contrast (~0.15) in the raw image. After the uniform background subtraction, the average contrast of Fig. 6 (b), defined as $\left(\overline{I}_{sig} - \overline{I}_{bg}\right) / \left(\overline{I}_{sig} + \overline{I}_{bg}\right)$, is found to be about 0.75 where $\overline{I}_{sig}$ and $\overline{I}_{bg}$ are the average signal and background intensities.

Another important factor is the signal-to-noise ratio (SNR) of the system. To estimate the SNR, we first divided the total imaging area into signal area and background area based on the guide of Fig. 6 (a): the bright area in Fig. 6 (a) was defined as the signal area, while the dark area was defined as the background area. The defined signal and background areas were overlaid onto Fig. 6 (b). We then calculated the average SNR as the ratio between the average intensity in the signal area in Fig. 6 (b) and the standard deviation in the background area in Fig. 6 (b). The average SNR was found to be about 8.5. The SNR was limited by the presence of noise due to the random fluctuation in the diffusive background. Notice that the DPC was performed with a phase-only SLM. By using a complex (amplitude and phase) SLM, we expect the intensity of the diffusive background can be further suppressed, and the contrast and SNR of the imaging will be greatly improved.

#132231 - $15.00 USD Received 26 Jul 2010; revised 5 Sep 2010; accepted 8 Sep 2010; published 15 Sep 2010

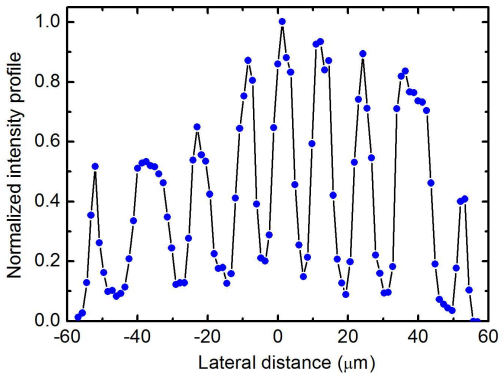

Fig. 7. The normalized intensity profile along the dashed line in the phase-conjugate scanning image shown in Fig. 6 (b). The experimental data points are shown as blue dots.

Conclusion

In conclusion, we demonstrated a phase-conjugate scanning microscopy which allows us to image through a thin turbid medium. We showed that the phase-conjugated focus can be scanned over 220 μm on the sample. We scanned the area around the SHRIMP in the two transverse directions but it is possible to scan the beam in the longitudinal direction as well by appropriately modifying the phase wave front on the SLM. While we demonstrated the phase-conjugate scanning microscopy with transmission detection, it can be easily extended to fluorescence microscopy. The phase-conjugated scanning focus can excite fluorescent probes and the fluorescent signal can be collected both in the transmission through clear media or in the epi-direction through the turbid medium. Two-photon fluorescence microscopy coupled with three-dimensional (3D) scanning can provide a 3D visualization of the volume surrounding each SHRIMP. Larger imaging coverage can be achieved by sequentially using multiple SHRIMP beacons and imaging the volumes around them. It is possible to illuminate the SHRIMPs at the fundamental frequency through the turbid medium rather than from the back-side as was done in these experiments. It will result in the illumination on the SHRIMPs being a speckle pattern, requiring fine scanning to locate individual SHRIMPs. The excitation intensity will also decrease significantly due to the scattering. This can be partially compensated by using brighter SHRIMP beacons with higher SHG efficiency [23,24]. Finally, the technique we demonstrated is applicable to relatively thin scattering media. We expect some real application such as imaging crustaceans, eggs, or blood vessels, where the imaging targets are surrounded by non-diffusive matters that are hidden by thin diffusive layers. As the thickness of the scattering region increases, the field of view decreases proportionally. Extension of this imaging technique to thicker scattering media remains a challenge.

Acknowledgements

The authors thank Dr. Paul Bowen at EPFL for providing the $BaTiO_3$ nanoparticles. This project is supported by the National Center of Competence in Research (NCCR), Quantum Photonics.

#132231 - $15.00 USD Received 26 Jul 2010; revised 5 Sep 2010; accepted 8 Sep 2010; published 15 Sep 2010